

IMAGING SPECTROMETRY AND METAMORPHIC PROCESSES

Edward F. Duke and Patrick K. Kozak¹

1. Introduction

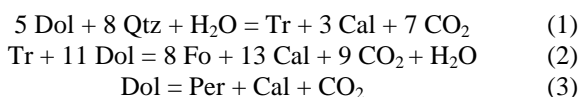
Metamorphism of rocks in the earth's crust is characterized by progressive changes in mineral assemblages, mineral proportions, and mineral chemistry in response to changes in temperature, pressure, or composition of coexisting fluids. Spectral features in the 0.4-2.5 μm wavelength range of modern imaging spectrometers serve to distinguish among important metamorphic minerals and, in some cases, to record the extent of temperature-sensitive cation exchange reactions. It is possible, therefore, to apply imaging spectrometer data to map the zonation of metamorphic minerals as a function of past thermal and compositional gradients in the crust.

The present study is part of a broader investigation, which examines the use of laboratory, field, airborne, and spaceborne spectroscopic measurements to achieve a better understanding of metamorphic conditions and metamorphic fluid flow. The emphasis is on field and laboratory visible and near infrared reflectance spectra, combined with high spectral resolution remote sensing imagery from NASA's Airborne Visible and Infrared Imaging Spectrometer (AVIRIS) and other imaging spectrometer data. In order to illustrate these applications, this paper presents AVIRIS images which delineate metamorphic zones resulting from contact metamorphism of siliceous dolomite near Ubehebe Peak, Death Valley National Park, California.

2. Geologic Setting

The Ubehebe Peak contact aureole is located in Death Valley National Park, California, at the southern end of the Last Chance Mountains (Fig. 1). Intrusion of Middle Jurassic (173 Ma) quartz monzonite into steeply dipping siliceous dolomites produced a zone of contact metamorphism that is well exposed for a distance of at least 2.5 km north of the intrusive (Roselle, 1997; Roselle et al., 1999). Metamorphic effects are most pronounced in the Silurian Hidden Valley dolomite and Devonian Lost Burro formation (McAllister, 1955, 1956), which are predominantly quartz-poor dolomite, with subordinate dolomitic sandstone and limestone layers. Approximately 5 km north of the intrusive body at Ubehebe Peak, another intrusive is exposed; although no detailed study of metamorphism has been conducted in that area, the intrusive is known to have caused local contact metamorphic effects and mineralization (McAllister, 1955, 1956; Burchfiel, 1969).

A comprehensive study of contact metamorphism at Ubehebe Peak was conducted by G.T. Roselle between 1992-1997 (Roselle, 1997, Roselle et al., 1999). That effort included detailed field mapping and air photo interpretation, and petrographic, petrologic, statistical, and stable isotopic analyses on 357 samples from the aureole. Metamorphic phase relations in the siliceous dolomites in the Ubehebe Peak aureole can be approximated by the simple CaO-MgO-SiO₂ (H₂O-CO₂) compositional system (Tracy and Frost, 1991). Roselle (1997) divided the aureole into an unmetamorphosed zone followed sequentially by tremolite, forsterite, and periclase zones toward the intrusive contact. A restricted wollastonite zone in calcitic marbles in the southwestern part of the aureole is shown in Figure 1, but not discussed further here. Reactions at the tremolite, forsterite, and periclase isograds can be approximated as follows (see Table 1 for mineral compositions and abbreviations):



¹ South Dakota School of Mines and Technology, Rapid City, SD 57701-3995, U.S.A. (edward.duke@sdsmt.edu)

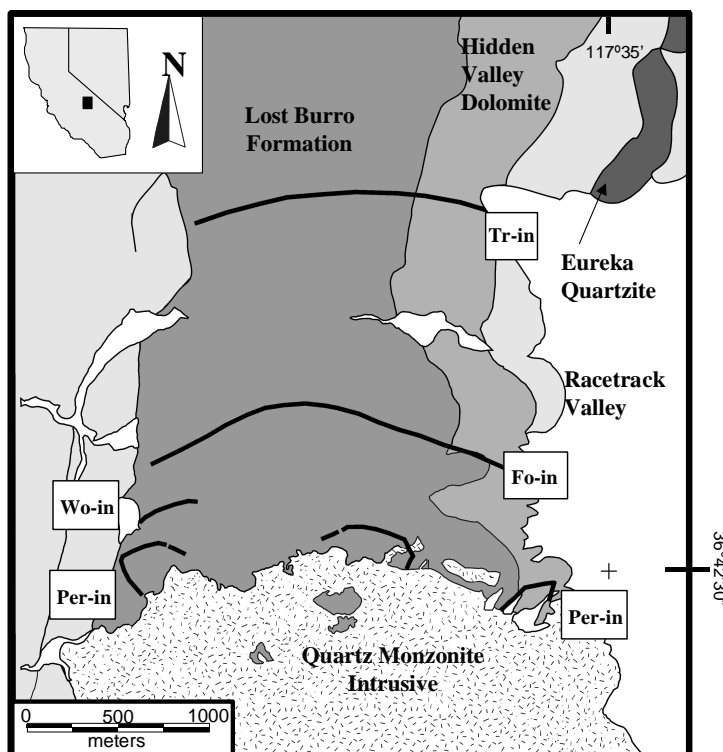
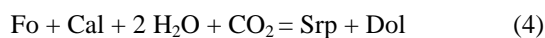


Figure 1. Generalized geologic map of the Ubehebe Peak contact aureole showing isograds (Roselle et al., 1999). (See Table 1 for mineral abbreviations.) Subsequent AVIRIS imagery covers most of this area with the exception of the western margin of map but extends roughly 3 km further north.

Retrograde effects resulted in partial alteration of the forsterite to serpentine and the complete replacement of periclase by brucite according to the following reactions:



Roselle et al. (1999) estimated the pressure of metamorphism at 1.4-1.7 kbar based on stratigraphic reconstructions. Temperatures of metamorphism, based on calcite-dolomite geothermometry, ranged from <300°C in the unmetamorphosed rocks to 665°C at the periclase isograd.

Table 1. Mineral abbreviations and chemical formulae

Dol = dolomite, $\text{CaMg}(\text{CO}_3)_2$	Fo = forsterite, Mg_2SiO_4
Cal = calcite, CaCO_3	Per = periclase, MgO
Qtz = quartz, SiO_2	Srp = serpentine, $\text{Mg}_3\text{Si}_2\text{O}_5(\text{OH})_4$
Tr = tremolite, $\text{Ca}_2\text{Mg}_5\text{Si}_8\text{O}_{22}(\text{OH})_2$	Brc = brucite, $\text{Mg}(\text{OH})_2$

3. Remote Sensing Data and Processing Methods

Airborne Visible and Infrared Imaging Spectrometer (AVIRIS) data used in this study were acquired May 3, 1996 (site name: Ubehebe west), and obtained for this project from NASA's Jet Propulsion Laboratory. The AVIRIS instrument platform is flown on a ER-2 at an altitude of 60,000 feet giving a spatial resolution of 20 m. The spectral data comprise 224 contiguous bands covering the wavelength range from 0.37 to 2.51 μm with bandwidth varying between approximately 8.5 and 11 nm. AVIRIS calibrated radiance values were corrected for atmospheric effects and converted to apparent reflectance using the ATREM procedure (Gao and Goetz, 1990).

Additional surface calibration of ATREM reflectance values was performed using an Empirical Line calibration method; field and laboratory reflectance spectra from sites within the image were used to determine gains and offsets for the image spectra (Kruse et al., 1990). In this study, laboratory spectra of samples from the quartz monzonite and the Racetrack Playa were used to set the dark and bright signals, respectively.

AVIRIS apparent surface reflectance images were analyzed using ENVI software. A Minimum Noise Fraction transformation was employed to determine a reduced set of noise-free spectral bands. Using the reduced set of bands, the Pixel Purity Index (Boardman et al., 1995) was used to identify spectrally pure pixels in the image. Spectra from these pixels were compared with field and laboratory spectra and with spectra from the U.S. Geological Survey spectral library (Clark et al., 1993) to derive a set of image-based spectral endmembers. Based on these endmembers, mineral maps of the distribution and relative abundance of important metamorphic minerals were generated using four different algorithms: Spectral Angle Mapper (SAM, Boardman and Kruse, 1994), Mixture Tuned Matched Filtering (MTMF, Boardman et al., 1995), Spectral Feature Fitting (Clark et al., 1990), and Linear Spectral Unmixing (LSU, Boardman, 1989). Examples of MTMF, LSU, and SAM results are presented in this paper.

In order to establish ground-truth data, over 1000 field and laboratory reflectance measurements in the spectral range 0.35-2.5 μm were acquired from the Ubehebe Peak contact aureole using a FieldSpec FR spectroradiometer from Analytical Spectral Devices (Boulder, CO). Mineral assemblages indicated by spectroscopic methods were evaluated by comparison with reference spectral libraries and validated using standard laboratory techniques including optical microscopy, scanning electron microscopy and energy-dispersive X-ray microanalysis, and X-ray diffraction.

4. Results

Field and laboratory spectra of samples from the Ubehebe Peak contact aureole are consistent with mixtures of the key CaO-MgO-SiO₂ (H₂O-CO₂) minerals listed in Table 1. Spectral features of calcite and/or dolomite dominate in most samples and features of tremolite and brucite are prominent locally. Quartz cannot be identified spectrally in the visible-near infrared, and the presence (or former presence) of forsterite is implied by strong spectral features of serpentine, which is a ubiquitous retrograde alteration product of forsterite. Other minerals recorded in spectra from the area include phlogopite (KMg₃AlSi₃O₁₀(OH)₂), which indicates some deviation from the simple CaO-MgO-SiO₂ (H₂O-CO₂) system, and scapolite (~Ca₄Al₆Si₆O₂₄(CO₃)) and chondrodite (Mg₅(SiO₄)₂(F,OH)₂), which indicate local metasomatism by igneous fluids. Grossular, epidote, malachite, and azurite were also identified in some samples.

The AVIRIS apparent reflectance spectra generally show excellent correlation with the field and laboratory data. Image-derived spectral endmembers are shown in Figure 2, in which it can be seen that most endmembers have diagnostic spectral features in wavelengths between 2.0 and 2.5 μm . The endmembers features can be correlated with spectral features of calcite (2.335 μm), dolomite (2.315 μm), tremolite (2.380 μm), and serpentine (2.216 μm). A satisfactory image endmember for brucite is difficult to determine for two reasons. First, the main spectral features of brucite are centered in the water-vapor absorption regions near 1.4 and 1.9 μm . Second, the periclase zone where brucite occurs is very limited in extent and generally less than 100 m wide (Fig. 1). Despite these problems, a distinct image endmember was derived, which contains a very minor feature at 0.956 μm , the wavelength of a second-order OH absorption in brucite. Although not discussed here, additional image endmembers were derived for Eureka quartzite and the quartz monzonite intrusive.

Figures 3-6 compare mineral maps for calcite, dolomite, tremolite, and serpentine derived using the LSU and MTMF algorithms. The first indication of significant amounts of tremolite (Fig. 3) corresponds very closely with the position of the tremolite-in isograd mapped by Roselle (1997) on the basis of field studies and petrographic analysis. Furthermore, the tremolite maps show that the distribution is highly irregular within the zone and probably related to stratigraphic variations in bulk composition of the dolomites. Most notably, tremolite is preferentially developed at a stratigraphic horizon representing the contact between the Hidden Valley dolomite and the Lost Burro formation. This so-called "gray layer" is a sandy dolomite with 5-10% quartz; it was the focus of much of the sampling and petrologic analysis by Roselle (1997) because the bulk composition resulted in the most complete sequence of the metamorphic reactions in the CaO-MgO-SiO₂ (H₂O-CO₂) system. Baumgartner et al. (1996)

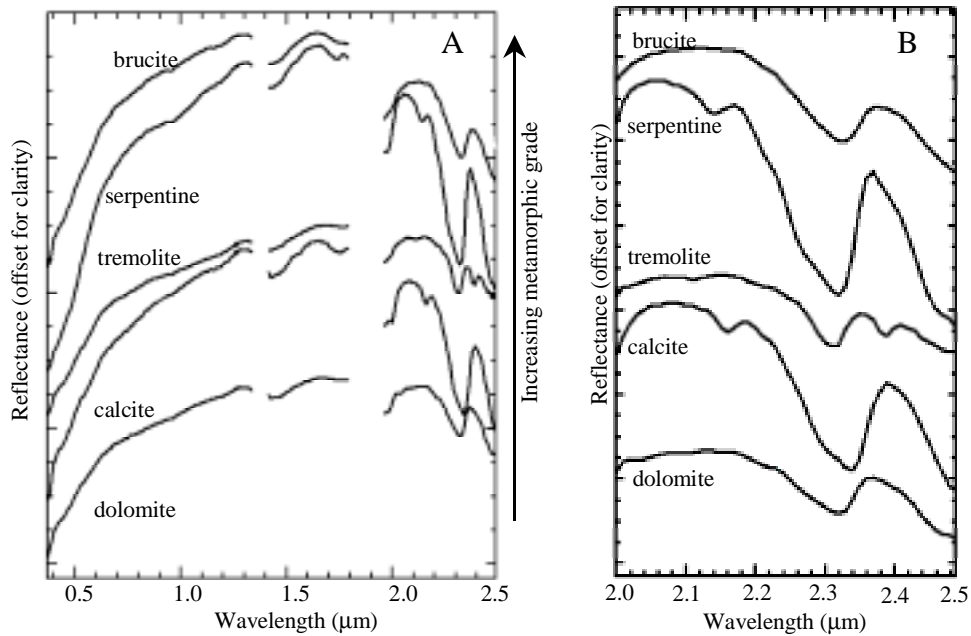


Figure 2. Endmember spectra derived from AVIRIS image labeled with corresponding mineral names. A) Full AVIRIS spectral range with atmospheric absorption regions masked near 1.4 and 1.9 μm . B) Expanded view of spectral features between 2.0 and 2.5 μm .

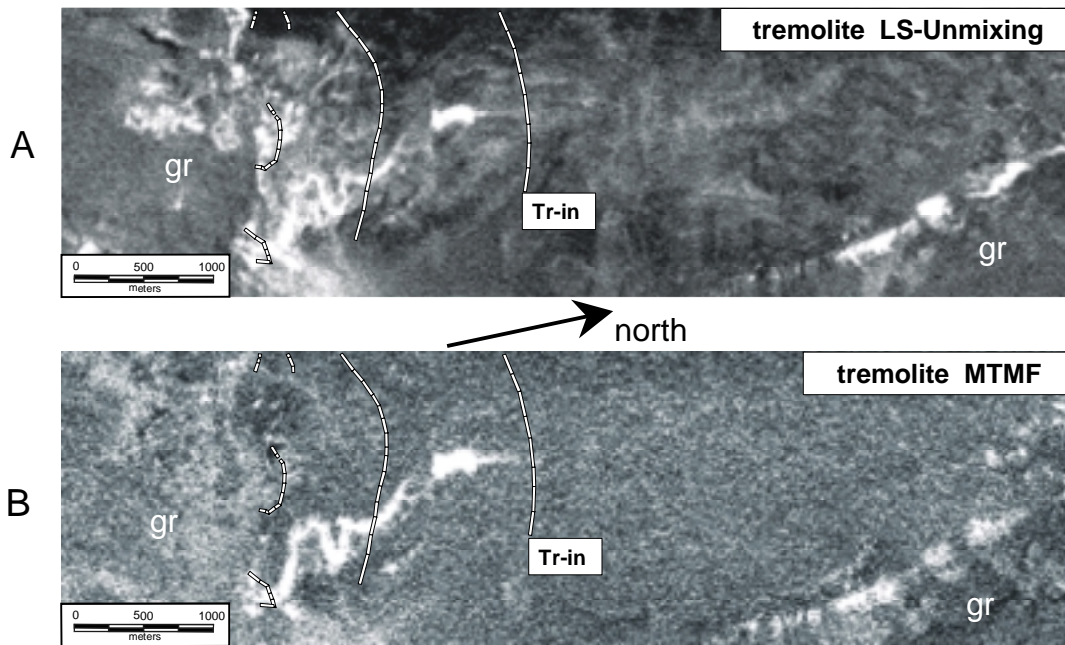


Figure 3. Maps of tremolite distribution based on A) Linear Spectral Unmixing and B) Mixture Tuned Matched Filtering. Higher abundances shown by brighter pixels. Tremolite (Tr) isograd from Roselle et al. (1999). Area covered by Fig. 1 includes only southern half of image. Note previously undefined zone of tremolite near granitic intrusive (gr) in the north.

suggested also that fracture-controlled infiltration of H_2O -rich fluids may have been focused selectively along beds in this layer. The presence of tremolite in screens and inliers within the quartz monzonite stock is indicated by the

LSU image but is less evident in the MTFM map. The distribution within the stock has not yet been tested by field studies.

The detailed mapping and petrologic interpretation by Roselle (1997) was restricted to the southern half of the area shown in Figures 3-6. The results of the hyperspectral analysis presented here show a previously undefined tremolite zone in the northern part of Figure 3 that is spatially associated with a poorly exposed granitic intrusive (McAllister, 1956; Burchfiel, 1969). The distribution of tremolite in those images suggests that it is developed primarily in the Pogonip limestone, and that the isograd may extend as far as 1-2 km from the closest exposure of the intrusive.

The serpentine images (Fig. 4) are considered to represent the extent of prograde forsterite, because most forsterite is partially or completely retrograded to serpentine by reactions such as (4), above. The maps indicate that serpentine is widely distributed within a zone extending roughly 800 meters from the intrusive contact, in close agreement with the position of the forsterite isograd as located by Roselle (1997). As in the case of tremolite, a previously unrecognized forsterite zone is also indicated adjacent to the intrusive in the northern part of the images. Reconnaissance sampling and laboratory spectral analysis showed that serpentine is indeed a major constituent of many rocks in that area. As in the southern part of the images, the serpentine in the north is in closer proximity to the intrusive than tremolite (mostly within 600 meters). The geology near the northern intrusive is more complicated than in the Ubehebe Peak aureole, and it appears that the development of serpentine is most pervasive in the Ordovician Ely Springs formation and Silurian Hidden Valley dolomite.

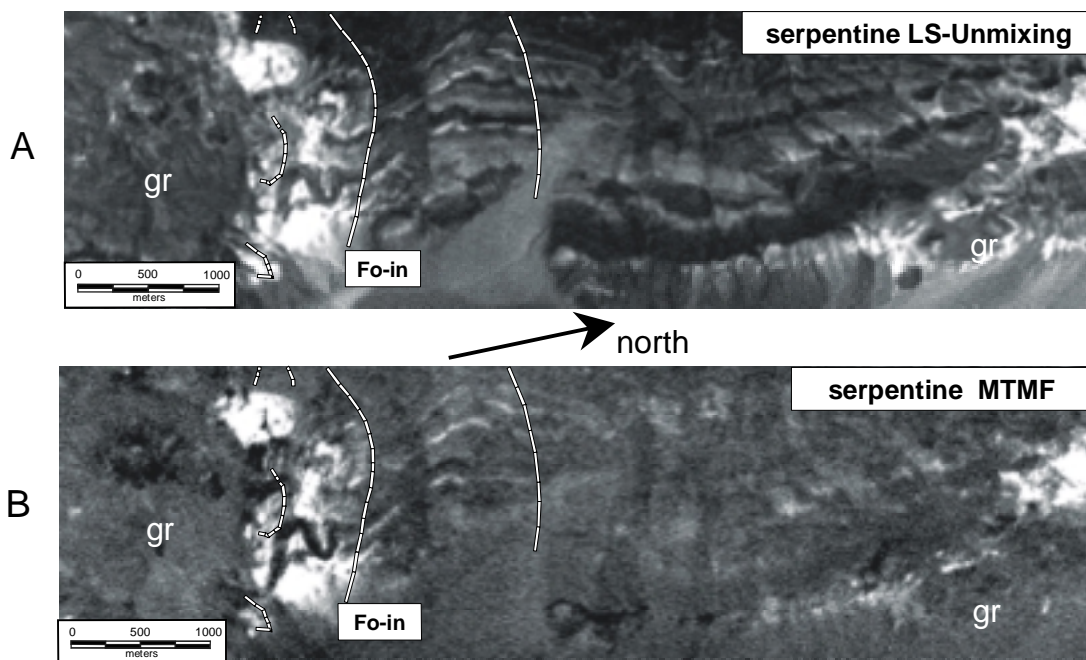


Figure 4. Maps of serpentine distribution based on A) Linear Spectral Unmixing and B) Mixture Tuned Matched Filtering. Higher abundances shown by brighter pixels. Serpentine distribution (retrograde) correlates with that of prograde forsterite as discussed in text. Forsterite (Fo) isograd from Roselle et al. (1999). Note previously undefined zone of serpentine (after forsterite) near granitic intrusive (gr) in the north.

Roselle et al. (1999) cited several lines of evidence for limited and spatially heterogeneous infiltration of H₂O-rich fluid in the contact aureole at Ubehebe Peak. Stable isotope depletions in calcite and dolomite ($\delta^{13}\text{C}$ as low as -9.1‰ and $\delta^{18}\text{O}$ as low as 11.1‰) were interpreted as one consequence of interaction with magmatic fluids. Isotopic depletions occur only in a zone 850 meters from contact, and within that zone only about one quarter of the samples showed evidence of isotopic exchange. This distribution coincides approximately with that of the forsterite

zone as delineated from the AVIRIS data. Although a theoretical or mechanistic basis for this apparent correspondence is not proposed here, it is possible that imaging spectrometer data may serve to outline zones of focused fluid flow and provide guidance for detailed field work and sampling for isotopic analysis.

The brucite images (Fig. 5) are considered to represent the extent of prograde periclase, because periclase is completely retrograded to brucite by reaction (5), above. The brucite distribution maps are based on an extremely minor spectral feature near 0.956 μm in combination with a larger feature at 2.318 μm . In addition to being small, the 0.956- μm feature is also in a region of potential interference by atmospheric water vapor. For these reasons, the reliability of this endmember is still being evaluated. Despite these reservations, the distribution of the brucite in the AVIRIS scene corresponds very well with the distribution of brucite (after periclase) as determined by Roselle (1997). Both the LSU and the MTMF image accurately mark a prominent but discontinuous brucite-bearing zone that extends approximately 200 meters north of the intrusive contact. Field and laboratory spectra from that zone display near textbook examples of brucite absorption features. The LSU image appears to include significantly more spurious pixels (e.g., in the tremolite and unmetamorphosed zones) than does the MTMF image. Also the MTMF image maps widespread brucite in screens and inliers of metamorphic country rock within the intrusive in accordance with Roselle (1997).

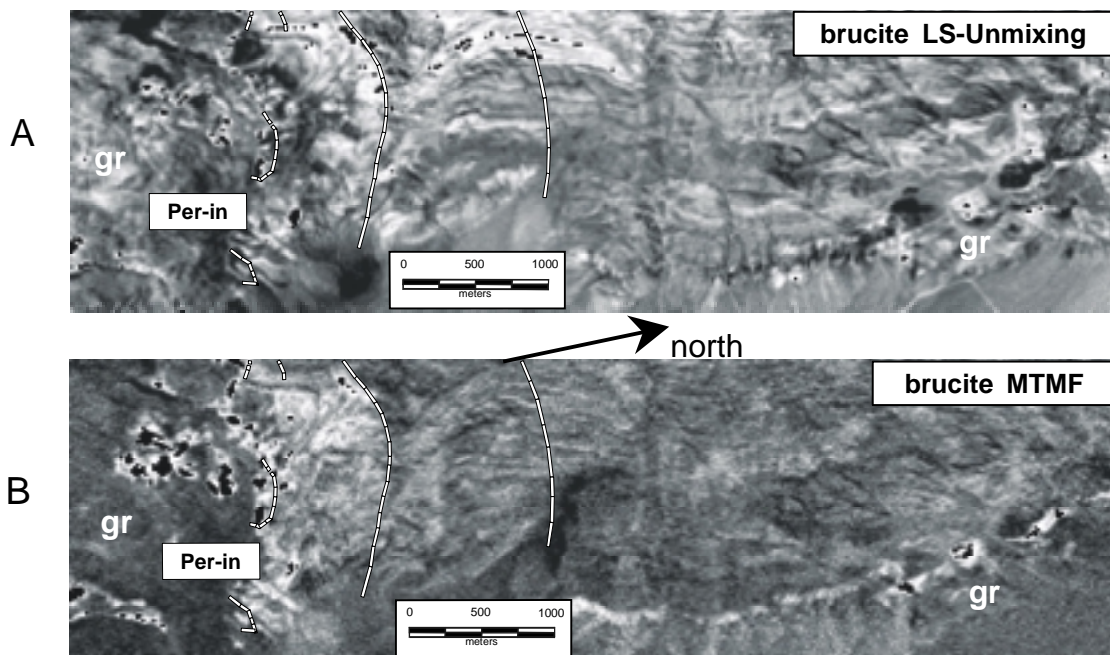


Figure 5. Maps of brucite distribution based on A) Linear Spectral Unmixing and B) Mixture Tuned Matched Filtering. In general, brighter pixels correspond to higher abundances; for clarity, however, pixels with maximum values are shown in black. Brucite distribution (retrograde) correlates with that of prograde periclase as discussed in text. Periclase (Per) isograd from Roselle et al. (1999). Note previously undefined zone of possible brucite (after periclase) near granitic intrusive (gr) in the north.

Spatial variability in the calcite/dolomite ratio within the AVIRIS scene is evident based on a shift of the main CO_3 band between 2.335 μm (calcite) and 2.315 μm (dolomite). Variation in the ratio may reflect a combination of initial sedimentological differences and the effects of the prograde metamorphic reactions (e.g., 1-3, above), all of which consume dolomite and produce calcite. Laboratory mixtures of pure calcite and dolomite indicate that this shift is not strictly linear with respect to the weight percentages but that it can be used to extract calcite/dolomite ratios with an accuracy of on the order of ± 10 percent. It should be cautioned, however, that tremolite, serpentine, and brucite have features between 2.297 and 2.324 μm , close to the main dolomite band.

Therefore, it may not be possible to use the CO₃ band shift to determine calcite/dolomite ratios in samples that contain abundant Mg-silicates or brucite.

The calcite maps (Fig. 6) show an increase in the abundance of calcite southward toward the intrusive contact, particularly above the forsterite isograd. Dolomite maps (not shown here) show a corresponding decrease in the abundance of dolomite with increasing metamorphic grade. A comparable zone of high calcite and low dolomite is also indicated adjacent to the intrusive body 5 km north of the Ubehebe Peak contact, although the distribution of isograds around the northern pluton has not been established by field studies.

Increase in the calcite/dolomite ratio with proximity to the two intrusives is further highlighted in Figures 7 and 8. Figure 7 compares the SAM rule images for dolomite and calcite and an image that represents the ratio of the calcite rule value divided by the dolomite rule value. Using this presentation, a major increase in the calcite/dolomite ratio is indicated near the Ubehebe Peak pluton in the south and the unnamed intrusive in the north.

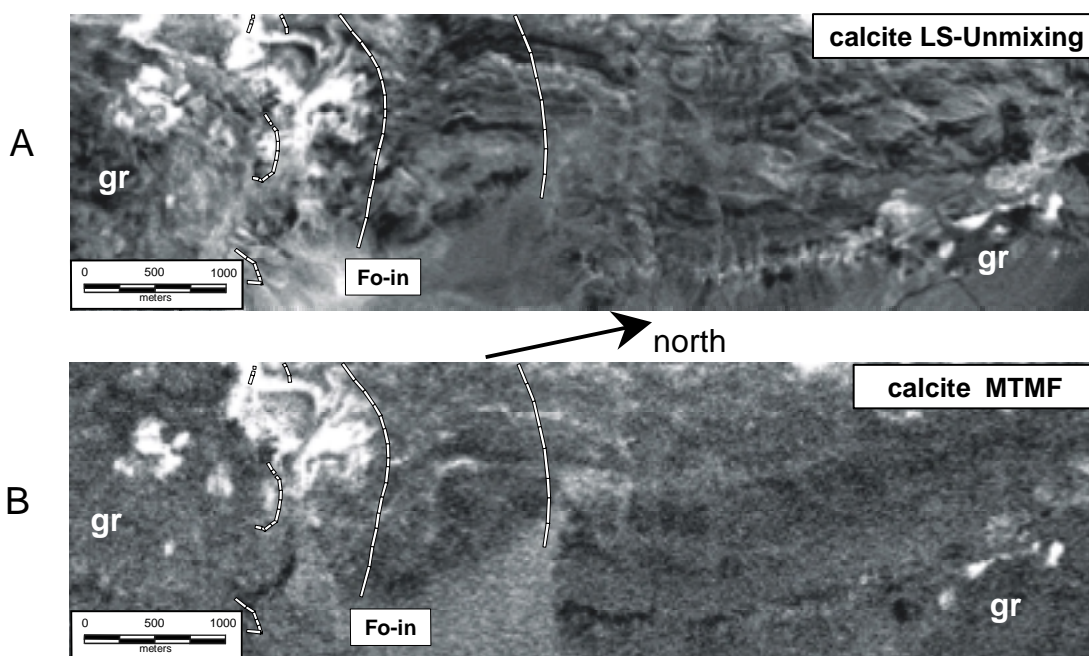


Figure 6. Maps of calcite distribution based on A) Linear Spectral Unmixing and B) Mixture Tuned Matched Filtering. Higher abundances shown by brighter pixels. Calcite abundance increases markedly above the forsterite isograd. Forsterite (Fo) isograd from Roselle et al. (1999). Note previously undefined zone of increased calcite abundance near granitic intrusive (gr) in the north.

Figure 8 shows a transect of SAM rule values southward through the Ubehebe Peak aureole, from the unmetamorphosed zone to the contact, along the lines shown in Figure 7. Calcite and dolomite rule values are relatively constant and positively correlated through the unmetamorphosed zone and tremolite zone. At the forsterite isograd, the two trends diverge: calcite increases and dolomite decreases at the same point that serpentine (after forsterite) increases. Calcite appears to increase through the forsterite zone, but very close to the contact, approximately coincident with the periclase isograd, the trends appear to reverse with an apparent increase in dolomite. This may reflect the fact that brucite (after periclase) has a spectral feature located at approximately the same wavelength as that of dolomite; if that is the case, the SAM values would no longer provide accurate estimates of the relative ratio of calcite and dolomite.

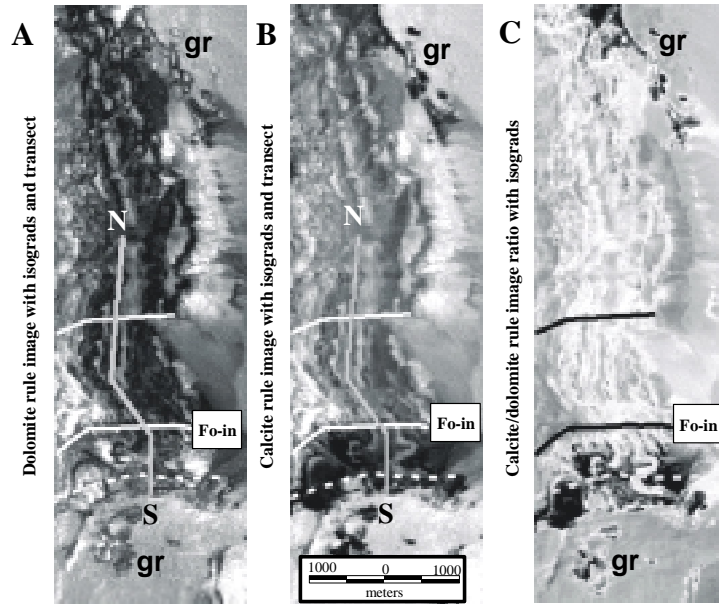


Figure 7. Spectral Angle Mapper rule images for A) dolomite, B) calcite, and C) calcite/dolomite ratio. Higher rule values shown in black. Forsterite (Fo) isograd from Roselle (1997). Note zones of high calcite and low dolomite near granitic intrusives (gr) in both the south and north parts of image. Line N-S shows location of transect in Fig. 8. (From Kozak and Duke, 2000.)

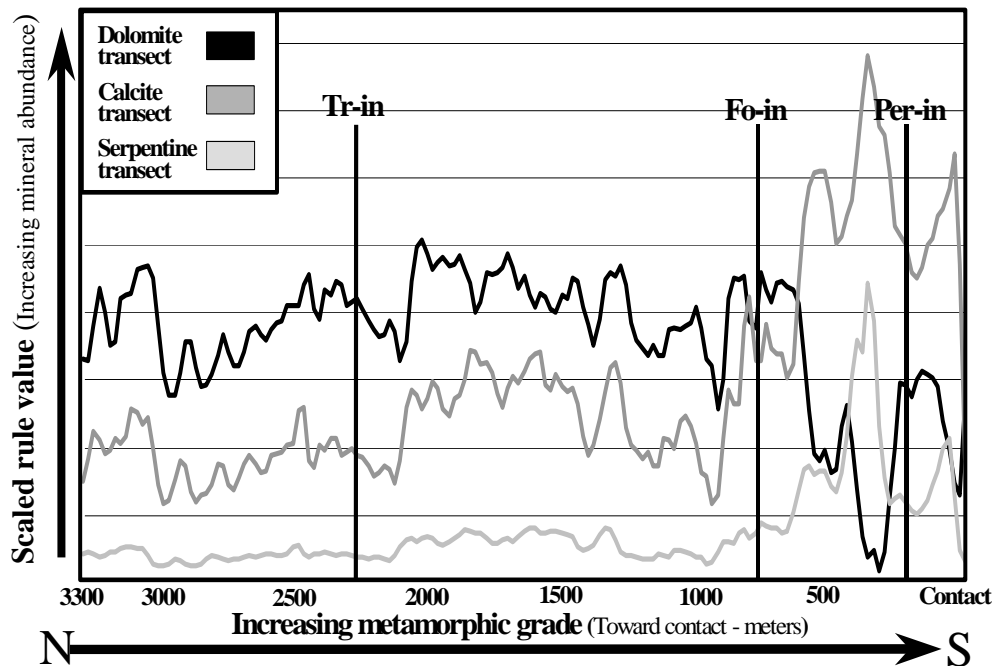


Figure 8. Variation of Spectral Angle Mapper rule values for dolomite, calcite, and serpentine along north to south transect through Ubehebe Peak aureole. Isograds from Roselle (1997). Transect location shown in Fig. 7. (From Kozak and Duke, 2000.)

5. Summary and Conclusions

The distribution of five key metamorphic minerals in the Ubehebe Peak contact aureole has been mapped with 20-meter spatial resolution based on AVIRIS imagery. At distances greater than 2.5 km from the intrusive contact the principal spectral feature in the rocks is that of dolomite. Within 2 km of the contact spectral features of tremolite occur. Within 800 meters of the contact spectral features of serpentine (retrograded forsterite) appear accompanied by a strong increase in the calcite/dolomite ratio. Locally, within 200 meters of the contact, spectral features attributed to brucite (retrograded periclase) are present in the AVIRIS image.

The isograd pattern determined from the AVIRIS spectral data is in excellent agreement with that of previous workers and with phase relations in metamorphosed siliceous dolomites. Moreover, the AVIRIS images reveal a previously unmapped contact aureole 5 km north of Ubehebe Peak and, although not discussed here, a third contact aureole is indicated, located on the east side of Racetrack Valley. The 20-m spatial resolution of the AVIRIS imagery also highlights the extremely irregular distribution of metamorphic minerals within their respective metamorphic zones, which is related to compositional layering in the dolomites and perhaps to localized fluid infiltration.

This work establishes the utility of imaging spectrometry as method for studying the metamorphism of impure carbonate rocks. A critical step in such studies is determining the spatial distribution of key metamorphic minerals as well as variations in their relative abundance. With the exception of tremolite, most of the metamorphic minerals mapped here using the AVIRIS data are extremely difficult to recognize in the field. For example, brucite and serpentine are difficult to identify, and distinguishing ratios of calcite and dolomite in mixed carbonates requires laboratory methods.

In the future, studies using even higher spatial resolution imaging spectrometer data (3-5 meters) will provide metamorphic petrologists with unprecedented insights into thermal, structural, and fluid evolution processes in contact aureoles.

6. Acknowledgments

Research on spectroscopic methods for mapping metamorphic rocks is supported by National Science Foundation grant EAR-9706629. AVIRIS data for graduate research was provided to PKK by NASA's Jet Propulsion Laboratory. The cooperation of the U.S. Park Service, Death Valley National Park, is gratefully acknowledged. The authors also thank G.T. Roselle and L.P. Baumgartner for information on the Ubehebe Peak contact aureole.

7. References

- Baumgartner, L.P., M.L. Gerdes, M.A. Person, and G.T. Roselle, 1996, "Porosity and Permeability of Carbonate Rocks during Contact Metamorphism," in B. Jamtveit and B. Yardley, eds., *Fluid Flow and Transport in Rocks: Mechanisms and Effects*, Chapman and Hall, London, pp. 83-98.
- Boardman, J.W., 1989, "Inversion of Imaging Spectrometer Data using Singular Value Decomposition," *Proceedings, IGARRS '89, Twelfth Canadian Symposium on Remote Sensing*, vol. 4, pp. 2069-2072.
- Boardman, J.W., and F.A. Kruse, 1994, "Automated Spectral Analysis: a Geological Example using AVIRIS Data, North Grapevine Mountains, Nevada," *Proceedings of the Tenth Thematic Conference on Geological Remote Sensing*, Environmental Research Institute of Michigan, vol. 1, pp. 407-418.
- Boardman, J.W., F.A. Kruse, and R.O. Green, 1995, "Mapping Target Signatures via Pixel Unmixing of AVIRIS Data," *Summaries of the Fifth Annual JPL Airborne Earth Science Workshop*, JPL Publication 95-1, vol. 1, pp. 23-26.
- Burchfiel, B.C., 1969, "Geology of the Dry Mountain Quadrangle, Inyo County, California," *California Division of Mines and Geology, Special Report 99*, 19 p.
- Clark, R.N., A.J. Gallagher, and G.A. Swayze, 1990, "Material Absorption Band Depth Mapping of Imaging Spectrometer Data using the Complete Band Shape Least-Squares Algorithm Simultaneously Fit to Multiple Spectral Features from Multiple Materials," *Proceedings of the Third Airborne Visible/Infrared Imaging Spectrometer (AVIRIS) Workshop*, JPL Publication 90-54, pp. 176-186.

- Clark, R.N., G.A. Swayze, A. Gallagher, T.V.V. King, and W.M. Calvin, 1993, "The U.S. Geological Survey, Digital Spectral Library. Version 1: 0.2 to 3.0 Micrometers," U.S. Geological Survey Open-File Report 93-592, 1326 pp.
- Gao, B.-C., and A.F.H. Goetz, 1990, "Column Atmospheric Water Vapor and Vegetation Liquid Water Retrievals from Airborne Imaging Spectrometer Data," *Journal of Geophysical Research*, vol. 95, pp. 3549-3564.
- Kozak, P.K., and E.F. Duke, 2000, "Hyperspectral Remote Sensing and Metamorphic Petrology: an Example from Contact Metamorphism at Ubehebe Peak, California," *GeoCanada 2000*, in review.
- Kruse, F.A., K.S. Kierein-Young, and J.W. Boardman, 1990, "Mineral Mapping at Cuprite, Nevada with a 63 Channel Imaging Spectrometer," *Photogrammetric Engineering and Remote Sensing*, vol. 56, pp. 83-92.
- McAllister, J.F., 1955, "Geology of Mineral Deposits in the Ubehebe Peak Quadrangle, Inyo County, California," California Division of Mines and Geology, Special Report 42, 63 p.
- McAllister, J.F., 1956, "Geology of the Ubehebe Peak Quadrangle, California," U.S. Geological Survey Map GQ-95, scale, 1:62,500.
- Roselle, G.T., 1997, "Integrated Petrologic, Stable Isotopic, and Statistical Study of Fluid-Flow in Carbonates of the Ubehebe Peak Contact Aureole, Death Valley National Park, California," Unpublished Ph.D. Dissertation, University of Wisconsin, Madison, WI.
- Roselle, G.T., L.P. Baumgartner, and J.W. Valley, 1999, "Stable Isotope Evidence of Heterogeneous Fluid Infiltration at the Ubehebe Peak Contact Aureole, Death Valley National Park, California," *American Journal of Science*, vol. 299, pp. 93-138.
- Tracy, R.J., and B.R. Frost, 1991, "Phase Equilibria and Thermobarometry of Calcareous, Ultramafic and Mafic Rocks, and Iron Formations," *Mineralogical Society of America Reviews in Mineralogy*, vol. 26, pp. 207-289.